

## 1 **Title**

2 Enhancing antibody responses by multivalent antigen display on thymus-independent DNA  
3 origami scaffolds

## 4 **Authors**

5 Eike-Christian Wamhoff<sup>1, \*</sup>, Larance Ronsard<sup>2, \*</sup>, Jared Feldman<sup>2, \*</sup>, Blake M. Hauser<sup>2, \*</sup> Grant A.  
6 Knappe<sup>1,3</sup>, Anna Romanov<sup>1,4</sup>, Evan Lam<sup>2</sup>, Kerri St. Denis<sup>2</sup>, Alejandro B. Balazs<sup>2</sup>, Aaron  
7 Schmidt<sup>2,5 \*\*</sup>, Daniel Lingwood<sup>2, \*\*</sup> and Mark Bathe<sup>1, \*\*</sup>

8

9 <sup>1</sup>Department of Biological Engineering, Massachusetts Institute of Technology, Cambridge, MA  
10 02139, United States

11 <sup>2</sup>Ragon Institute of Massachusetts General Hospital, Massachusetts Institute of Technology and  
12 Harvard University, Cambridge, MA 02139, United States

13 <sup>3</sup>Department of Chemical Engineering, Massachusetts Institute of Technology, Cambridge, MA  
14 02139, United States

15 <sup>4</sup>Koch Institute for Integrative Cancer Research, Massachusetts Institute of Technology,  
16 Cambridge, MA 02139, United States

17 <sup>5</sup>Department of Microbiology, Harvard Medical School, Boston, MA 02115, United States

18

19 \*These authors contributed equally

20 \*\*Correspondence to: [mark.bathe@mit.edu](mailto:mark.bathe@mit.edu), [dlingwood@mgh.harvard.edu](mailto:dlingwood@mgh.harvard.edu) or  
21 [aschmidt@crystal.harvard.edu](mailto:aschmidt@crystal.harvard.edu)

## 22 **Abstract**

23 Multivalent antigen display is a well-established design principle to enhance humoral immunity  
24 elicited by subunit vaccines. Protein-based virus-like particles (VLPs) are an important vaccine  
25 platform that implements this principle but also contain thymus-dependent off-target epitopes,  
26 thereby generating neutralizing and defocused antibody responses against the scaffold itself.  
27 Here, we present DNA origami as an alternative platform to display the receptor binding domain  
28 (RBD) of SARS-CoV-2. DNA-based scaffolds provide nanoscale control over antigen organization  
29 and, as thymus-independent antigens, are expected to induce only extrafollicular B-cell  
30 responses. Our icosahedral DNA-based VLPs elicited valency-dependent BCR signaling in two  
31 reporter B-cell lines, with corresponding increases in RBD-specific antibody responses following  
32 sequential immunization in mice. Mouse sera also neutralized the Wuhan strain of SARS-CoV-  
33 2—but did not contain boosted, DNA-specific antibodies. Thus, multivalent display using DNA  
34 origami can enhance immunogenicity of protein antigens without generating scaffold-directed  
35 immunological memory and may prove useful for rational vaccine design.

## 36 Introduction

37 The multivalent display of antigens at the nanoscale has been demonstrated to improve the  
38 immunogenicity of subunit vaccines<sup>1-3</sup>. Nanoparticulate vaccines with diameters between 20 and  
39 200 nm ensure efficient trafficking to secondary lymphoid organs<sup>4</sup>. In secondary lymphoid organs,  
40 high valency and avidity promote B-cell receptor (BCR) crosslinking and signaling as well as BCR-  
41 mediated antigen uptake, thereby driving early B-cell activation and humoral immunity<sup>5-12</sup>. The  
42 importance of BCR signaling for antibody responses was initially recognized for thymus-  
43 independent (TI) antigens, particularly of the TI-2 class<sup>13-15</sup>. The multivalent display of these non-  
44 protein antigens induces BCR crosslinking in the absence of T-cell help, ensuring that antibody  
45 responses proceed through extrafollicular B-cell pathways and thereby limiting germinal center  
46 (GC) reactions, affinity maturation and induction of B-cell memory<sup>16-17</sup>. Multivalent antigen display  
47 also enhances the BCR-mediated response to thymus-dependent (TD) antigens including  
48 proteins<sup>7-8</sup>. In this context, follicular T-cell help enables GC reactions to generate affinity-matured  
49 B-cell memory that can be boosted or recalled upon antigen reexposure<sup>18-20</sup>. Consequently, the  
50 nanoscale organization of antigens represents a well-established vaccine design principle, not  
51 only for TI antigens, but also to elicit humoral immunity through the TD pathway<sup>1-3</sup>.

52 Leveraging this design principle, native and engineered protein-based virus-like particles  
53 (P-VLPs) have emerged as an important platform for multivalent subunit vaccines<sup>21-36</sup>. P-VLPs  
54 enable the rigid display of antigens and have recently been used to investigate the impact of  
55 valency on B-cell activation *in vivo* to greater detail, suggesting differential regulation of affinity  
56 maturation and enhanced breadth of antibody responses at high valency<sup>7-9</sup>. However, valency  
57 control remains limited by the number of distinct protein components used for VLP assembly or  
58 by statistical functionalization with antigens—and is typically dependent on scaffold size and  
59 geometry. Notably, protein-based scaffolds are also TD antigens that elicit humoral immunity,  
60 including both T- and B-cell memory<sup>36-37</sup>. These scaffolds contain, and multivalently display, off-  
61 target epitopes that can defocus antibody responses, and such defocusing competes with the  
62 principles of rational vaccine design<sup>38-39</sup>. Scaffold-directed immunological memory can further  
63 complicate sequential or diversified immunizations with a given P-VLP, resulting in antibody-  
64 dependent clearance of the vaccine platform<sup>40-41</sup>.

65 We sought to address these limitations by combining rigid, multivalent antigen display with  
66 scaffolds composed of TI antigens. We hypothesized that such nanoscale organization could  
67 promote TD antibody responses against protein antigens but confine scaffold-directed B-cell  
68 responses to the non-boostable, extrafollicular pathway devoid of immunological memory.  
69 Wireframe DNA origami provides access to designer VLPs of controlled geometry and size at the  
70 20 to 200 nm scale with independently programmable geometry, valency and stoichiometry of  
71 antigen display<sup>42-46</sup>. We and others recently leveraged this platform to probe the nanoscale  
72 parameters of IgM recognition and of BCR signaling in reporter B-cell lines, suggesting that  
73 increased antigen spacing up to 30 nm promotes early B-cell activation<sup>47-48</sup>. However, these  
74 nanoscale design rules remain to be validated *in vivo*. While the utility of DNA-based VLPs (DNA-  
75 VLPs) to enhance antibody responses has not been demonstrated, DNA origami has been  
76 successfully employed to deliver therapeutic cargo to tumors in mice<sup>49-50</sup>. Other examples of *in*  
77 *vivo* delivery include the co-formulation of antigens and adjuvants to elicit T-cell immunity<sup>51</sup>.  
78 Importantly, and in contrast to P-VLPs, DNA-based scaffolds constitute TI antigens and should  
79 therefore be excluded from the boostable follicular pathway<sup>51-52</sup>.

80

81 As proof-of-concept, we report on the fabrication of DNA-VLPs functionalized with the  
82 SARS-CoV-2 receptor binding domain (RBD) derived from the spike glycoprotein, a key target for  
83 eliciting neutralizing antibodies against the virus<sup>53-56</sup>. Our nanoparticulate vaccine displayed  
84 enhanced binding to ACE2-expressing cells and induced valency-dependent BCR signaling *in*  
85 *vitro*. Following sequential immunization in mice, we observed corresponding valency-dependent  
86 enhancement of RBD-specific antibody responses and B-cell memory recall. Mouse sera also  
87 efficiently neutralized the Wuhan strain of SARS-CoV-2 for DNA-VLPs compared with monomeric  
88 RBD—but did not contain boosted, DNA-specific antibodies. Taken together, our findings suggest  
89 that DNA origami can be leveraged for multivalent antigen display without eliciting TD B-cell  
90 responses against the DNA-based scaffold, rendering this platform useful for rational vaccine  
91 design.

## 92 **Results and Discussion**

93 The spherical SARS-CoV-2 virion is approximately 100 nm in diameter and displays  
94 approximately 100 trimeric spike glycoproteins<sup>57</sup>. Each monomer contains the RBD which is  
95 essential for engaging the ACE2 receptor and viral uptake, rendering it a key target of neutralizing  
96 antibody responses<sup>53-56</sup>. We adapted our previous DAEDALUS design, an icosahedral DNA-VLP  
97 with 50 potential conjugation sites and approximately 34 nm in diameter, to display the RBD and  
98 investigate impact of nanoscale antigen organization by DNA origami on B-cell activation<sup>48</sup>. A  
99 covalent *in situ* functionalization strategy employing strain-promoted azide-alkyne cycloaddition  
100 (SPAAC) chemistry was used for antigen attachment (**Figure 1A**)<sup>44</sup>. Towards this end, we  
101 synthesized 30 oligonucleotide staples bearing triethylene glycol (TEG)-DBCO groups at their 5'  
102 ends to assemble DNA-VLPs symmetrically displaying 1x, 6x or 30x DBCO groups on their  
103 exterior (**Figure S1, Table S1 to S3**). Employing a reoxidation strategy, the RBD was selectively  
104 modified at an engineered C-terminal Cys with a SMCC-TEG-azide linker and subsequently  
105 incubated with DBCO-bearing DNA origami to fabricate **I52-1x-, 6x-, 30x-RBD (Figures 1B and**  
106 **S2, Note S1)**. The optimization of reaction conditions yielded near-quantitative conversion and  
107 coverage of more than 80% of conjugation sites on average as determined by denaturing,  
108 reversed-phase HPLC and Trp fluorescence (**Figures 1C and S3**). Notably, conversion was  
109 dependent on maximum DBCO concentrations and we obtained only up to 30% coverage for **I52-**  
110 **1x-RBD**. The monodispersity of purified DNA-VLPs was validated by dynamic light scattering  
111 (DLS) (**Figure 1D**). Analysis of **I52-30x-RBD** via negative-strain transmission electron microscopy  
112 (TEM) validated structural integrity of the DNA origami (**Figure 1E and S4**). While the icosahedral  
113 geometry could not be fully resolved, presumably due to accumulation of uranyl formate in the  
114 interior of the DNA origami, antigens were clearly visible and organized symmetrically.

115 To investigate the binding activity of RBD-Az before and after conjugation to DNA-VLPs,  
116 we conducted flow cytometry experiments with ACE2-expressing HEK293 cells (**Figure 2A**).  
117 Initially, monovalent binding of wild-type RBD and fluorophore-labeled RBD-Cy5, obtained by  
118 selectively labeling the azide, was compared (**Figure 2B and C**). The RBD constructs were  
119 incubated at 200 nM with the HEK293 cells and bound antigen was detected using the previously  
120 described anti-RBD antibody CR3022<sup>56</sup>. These experiments revealed comparable binding  
121 between the two constructs, demonstrating preservation of the receptor binding motif (RBM) and  
122 the viability of the reoxidation strategy for selective labeling of the terminal Cys (**Figure S2, Note**  
123 **S1**). Next, we explored whether multivalent RBD display using DNA-VLPs would result in  
124 increased avidity. Two additional fluorophore-labeled VLPs, **I52-30x-RBD-5x-Cy5** and **I52-5x-**  
125 **Cy5**, were synthesized to allow for direct detection of binding (**Figure 1B and S1**). Indeed, binding

126 of the RBD-functionalized VLPs was significantly enhanced compared to monomeric RBD-Cy5,  
127 while no binding was observed for the **I52-5x-Cy5 (Figure 2D and E)**. When correcting for Cy5  
128 brightness per RBD, **I52-30x-RBD-5x-Cy5** displayed approximately one order of magnitude  
129 higher median fluorescence intensity compared with monomeric RBD-Cy5, indicative of avidity  
130 effects for VLP recognition.

131 We then evaluated the capacity of RBD-functionalized DNA-VLPs to induce BCR signaling  
132 using a previously described  $\text{Ca}^{2+}$  flux assay (**Figure 2A**)<sup>58</sup>. Specifically, Ramos B-cell lines  
133 expressing the somatic CR3022 or B38 antibodies were established<sup>56, 59</sup>. BCR signaling was  
134 initially validated by incubation with an anti-IgM antibody. At 30 nM antigen, monomeric wild-type  
135 RBD did not elicit B-cell activation *in vitro* (**Figure 2F and G**). By contrast, incubation of the Ramos  
136 B cells with multivalent DNA-VLPs at the same antigen concentration resulted in efficient BCR  
137 signaling. We further observed valency-dependent increases in total  $\text{Ca}^{2+}$  flux for both cell lines  
138 with **I52-30x-RBD** being more potent than **I52-6x-RBD**. CR3022 ( $K_D = 0.27 \mu\text{M}$ , **Figure 2F**) and  
139 B38 ( $K_D = 1.00 \mu\text{M}$ , **Figure 2G**) bind distinct RBD epitopes with moderate monovalent affinity as  
140 reported for the corresponding Fab fragments<sup>60</sup>. Despite this 4-fold difference in affinity, we  
141 observed comparable total BCR signaling relative to the IgM control for all functionalized DNA-  
142 VLPs, consistent with previously described avidity effects at the B-cell surface<sup>61</sup>. We concluded  
143 that our DNA-VLPs efficiently interacted with and induced signaling by RBD-specific BCRs,  
144 analogous to previous studies using similar assays to evaluate multivalent subunit vaccines<sup>58, 62-</sup>  
145 <sup>68</sup>. The increased B-cell activation for **I52-30x-RBD** contrasts our previous findings for HIV  
146 antigens for which total  $\text{Ca}^{2+}$  flux saturated beyond a valency of  $10 \times 10^4$ . Notably, the antigen-BCR  
147 systems differ with respect to affinity and mode of antigen attachment: The affinity of the HIV  
148 antigen was substantially higher (eOD-GT8,  $K_D = 30 \text{ pM}$ ) and the antigens were non-covalently  
149 attached to DNA origami using rigid DNA-PNA duplexes.

150 Next, we investigated whether RBD-functionalized DNA-VLPs could activate B-cells *in vivo* and  
151 induce antibody responses. C57BL/6 mice were sequentially immunized with monomeric wild-  
152 type RBD, **I52-6x-RBD** and **I52-30x-RBD** at doses equivalent to  $7.5 \mu\text{g}$  RBD (**Figure 3A and S3**).  
153 IgG responses against the RBD were monitored throughout this regimen using ELISA and  
154 correlated with our *in vitro* BCR signaling findings (**Figure 3B and S5**). Post-boost 1, we observed  
155 an approximately 130-fold increase in endpoint dilutions for the 30-valent DNA-VLP over  
156 monomeric RBD. **I52-6x-RBD** did not enhance the B-cell response and elicited comparable  
157 antibody titers to monomeric RBD, both post-boost 1 and 2. Overall, endpoint dilutions were  
158 further increased post-boost 2 but converged between the groups. Earlier and stronger boosting  
159 of IgG titers and efficient B-cell memory recall is a hallmark of multivalent versus monomeric  
160 subunit vaccines<sup>22-23</sup>. Our findings are further consistent with enhanced IgG titers elicited by P-  
161 VLPs of increasing the valency<sup>7-9</sup>. Notably, we did not observe boosting of DNA-specific IgG titers  
162 against the scaffold, indicating an absence of B-cell memory for the DNA-VLP (**Figure 3C and**  
163 **S6**). While this finding was expected for TI antigens such as DNA, it was also established that TD  
164 antibody responses can be generated against TI antigens by covalent attachment to protein  
165 antigens<sup>69-70</sup>. The inverse case does not appear to be the default—scaffolding protein antigens  
166 with TI antigens does not direct the B-cell response to the extrafollicular pathway. By contrast, we  
167 observed valency-dependent TD antibody responses to the RBD, akin to virosomal and ISCOM-  
168 based vaccine design principles in which protein antigens are multivalently displayed by TI  
169 antigen-composed matrices<sup>71-74</sup>. The valency-dependent enhancement of RBD-specific antibody  
170 responses was further reflected in the efficient neutralization of the wild-type, Wuhan strain of

171 SARS-CoV-2 (**Figure 3D**)<sup>75-76</sup>. These findings suggest that immunization with **I52-30x-RBD** not  
172 only resulted in increased IgG titers but also induced functionally improved humoral immunity.

## 173 **Conclusions**

174 Here, we report on the use of wireframe DNA origami to program the display of SARS-CoV-2  
175 antigens. RBD-functionalized DNA-VLPs efficiently bound to the ACE2 receptor and activated B  
176 cells *in vitro*. BCR signaling increased with DNA-VLP valency and no saturation effects were  
177 observed for up to 30x RBD antigens. We further demonstrate the utility of DNA-VLPs as an *in*  
178 *vivo* platform for rational vaccine design. In particular, we provide proof-of-concept that multivalent  
179 DNA-VLPs can enhance TD antigen-specific humoral immunity in mice, but, as TI scaffolds, do  
180 not generate boostable B-cell memory against the vaccine platform itself. Because DNA origami  
181 also offers independent control over VLP size and geometry versus multivalent antigen display,  
182 DNA-based scaffolds may prove particularly useful if epitope focusing and nanoscale control are  
183 desired. By contrast, several P-VLPs explored as multivalent subunit vaccines against SARS-  
184 CoV-2 and other viruses elicit scaffold-directed humoral immunity<sup>30-31, 36-37</sup>—and the defocusing  
185 of RBD-specific antibody responses has been shown to reduce cross-neutralization of SARS-  
186 CoV-2 variants<sup>37</sup>.

187 Maintaining antigen display in B-cell follicles over time has been shown to promote GC reactions  
188 and humoral immunity<sup>77-78</sup>. While our findings suggest that non-protected, covalently  
189 functionalized DNA-VLPs are sufficiently stable to enhance antibody responses, it will thus be  
190 important to investigate to what extent multivalent antigen display is maintained in secondary  
191 lymphoid organs in the presence of nuclease degradation<sup>79-80</sup>. Trafficking to secondary lymphoid  
192 organs and B-cell activation might also be enhanced by varying DNA-VLP size and valency, for  
193 example to mimic SARS-CoV-2 virions<sup>57</sup>. Beyond vaccine design, our findings are of potential  
194 importance to gene therapy by addressing antibody-dependent clearance<sup>40-41</sup>—with DNA origami  
195 emerging as an alternative delivery platform<sup>81</sup>.

## 196 **Methods**

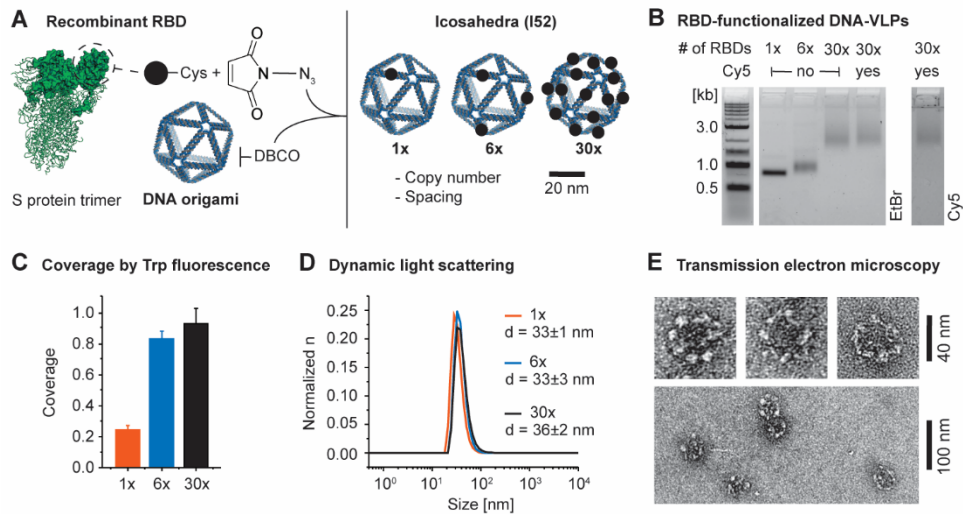
197 Methods are described in the **Supporting Information**.

## 198 **Acknowledgments**

199 E.-C.W., G.K., and M.B. were supported by NIH R21-EB026008, NSF CCF-1564025, CBET-  
200 1729397, and CCF-1956054, ONR N00014-21-1-4013 and N00014-17-1-2609, ARO ISN  
201 W911NF-13-D-0001, and Fast Grants Agreement EFF 4/15/20. E.-C. W. was additionally  
202 supported by the Feodor Lynen Fellowship of the Alexander von Humboldt Foundation. B.M.H  
203 was supported by NIGMS (T32GM007753) and F30 AI160908. J.F. was supported by NIGMS  
204 (T32AI007245). A.G.S. was supported by NIH (R01 AI146779) and a Massachusetts Consortium  
205 on Pathogenesis Readiness (MassCPR) grant. DL was supported by NIH (R01AI137057,  
206 R01AI153098, R01AI155447).

207

208 **Figures**

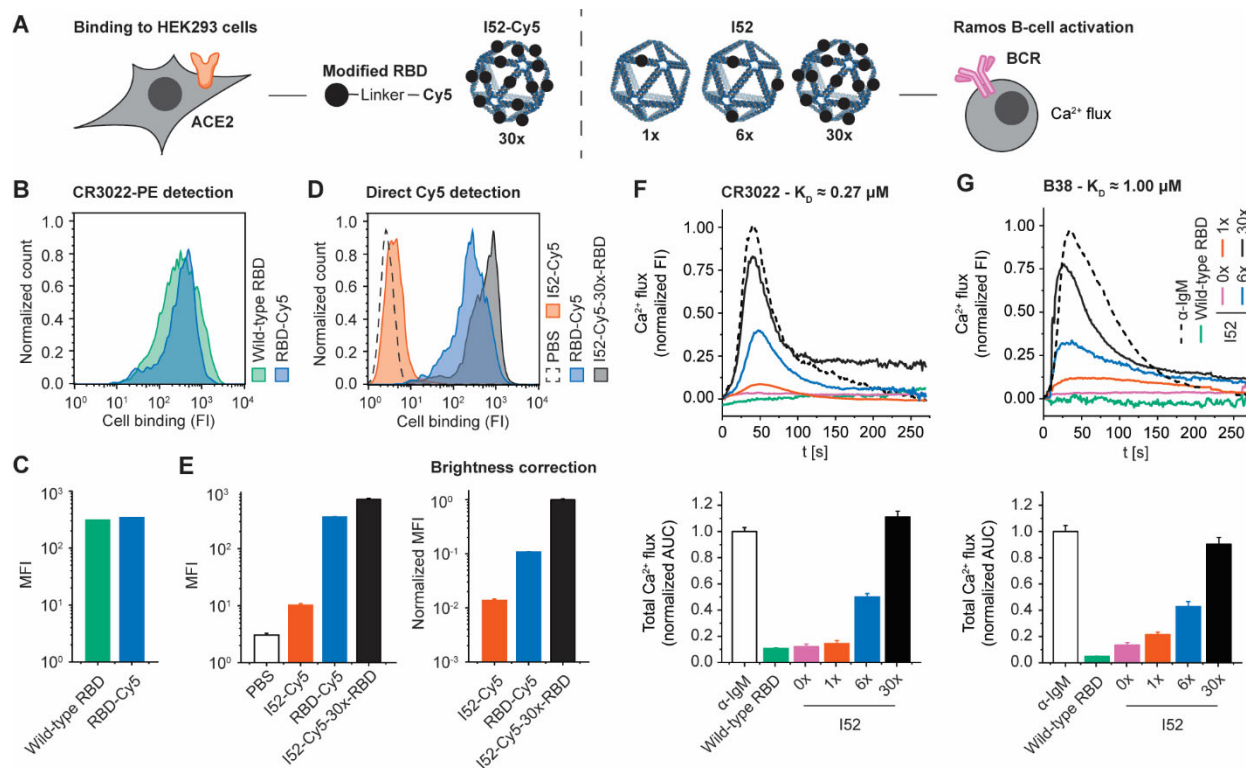


209

210 **Figure 1. Design and synthesis of DNA-VLPs covalently displaying the SARS-CoV-2 RBD.**

211 (A) Recombinant RBD bearing an additional Cys residue at the C-terminus was expressed. The C-terminal Cys was  
 212 selectively labeled with and SMCC-TEG-azide linker and subsequently conjugated to DBCO-bearing DNA-VLPs. The  
 213 icosahedral DNA origami objects of approximately 50 nm diameter displaying 1, 6 and 30 copies of the RBD were  
 214 fabricated. (B) Agarose gel electrophoresis (AGE) shows the gel shift due to increasing RBD copy number as well as  
 215 low polydispersity of the VLPs samples after purification. An additional VLP bearing 5 copies of Cy5 was produced for  
 216 ACE2-binding flow cytometry experiments. (C) The coverage of the DNA-VLPs with RBD was quantified via Trp  
 217 fluorescence. (D) Dynamic light scattering (DLS) was used to assess the dispersity of functionalized VLP samples.  
 218 Representative histograms are shown. (E) Transmission electron micrographs (TEM) of **152-30x-RBD** were obtained  
 219 by negative staining using 2% uranyl formate and validate the symmetric nanoscale organization of antigens. Coverage  
 220 values were determined from  $n = 3$  biological replicates for **152-1x-RBD** and from  $n = 6$  biological replicates for  
 221 **152-6x** and **30x-RBD**. Diameters were determined from 3 technical replicates.

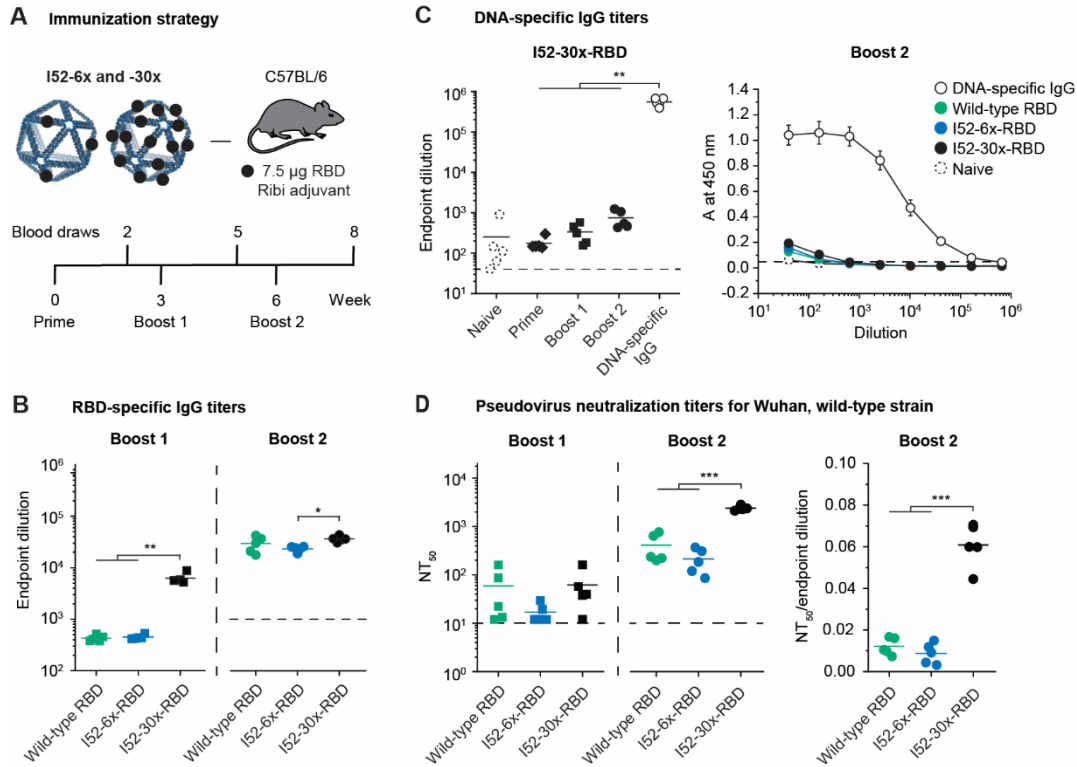
222



223

224 **Figure 2. In vitro activity of RBD-functionalized DNA-VLPs.**

225 **(A)** An overview of the in vitro activity assays and corresponding DNA-VLPs is shown. **(B and C)** ACE2-expressing  
 226 HEK293 cells were incubated with 200 nM RBD. Binding was detected in flow cytometry experiments using PE-labeled  
 227 CR3022 and a PE-labeled secondary antibody, demonstrating preserved binding activity for chemically modified RBD-  
 228 Cy5 compared to wild-type RBD. **(D and E)** Incubation with Cy5-labeled **I52-30x-RBD** at 100 nM RBD revealed  
 229 enhanced binding compared to RBD-Cy5 due to multivalency effects. No unspecific binding for non-functionalized **I52**  
 230 was observed. The brightness of Cy5-labeled **I52-30x-RBD** (5 Cy5 per 30 RBDs) and RBD-Cy5 (1 Cy5 per 1 RBD)  
 231 was quantified experimentally (**Figure S4**) and MFI values were corrected accordingly. **(F and G)** Ramos B cells  
 232 expressing the BCRs C3022 and B38 were incubated with α-IgM, wild-type RBD or RBD-functionalized DNA-VLPs at  
 233 30 nM RBD. Ca<sup>2+</sup> flux in response to RBD incubation was assayed using Fura Red. Representative fluorescence  
 234 intensity curves are shown (top). Total Ca<sup>2+</sup> flux was quantified via the normalized AUC, revealing robust activation of  
 235 BCR-expressing Ramos B cells by functionalized DNA-VLPs (bottom). No stimulation was observed for wild-type RBD  
 236 or for non-functionalized **I52**. Representative histograms are shown for ACE2 binding assays and MFI values were  
 237 determined from n = 3 biological replicates. Normalized AUC values were determined from n = 3 biological replicates.



238  
239  
240  
241  
242  
243  
244  
245  
246  
247  
248

**Figure 3. Antibody responses to RBD-functionalized DNA-VLPs.**

(A) Mice were immunized intraperitoneally with monomeric RBD and RBD-functionalized DNA-VLPs of varying copy number following a prime-boost-boost regimen. (B) RBD-specific IgG endpoint dilutions were determined via ELISA, revealing enhanced antibody responses for **I52-30x-RBD** compared to both monomeric RBD and **I52-6x-RBD**. (C) DNA-VLPs did not elicit enhanced DNA-specific IgG titers compared to monomeric RBD as measured by ELISA. Importantly, DNA-specific IgG were not increased after boost immunizations with DNA-VLPs. DNA-specific IgG was diluted from 10 µg/ml. (D) Serum neutralization titers expressed as NT<sub>50</sub> values against pseudoviruses modeling the wild-type, Wuhan strain were determined. We observed enhanced, valency-dependent neutralization efficiency for **I52-30x-RBD**. Mice were immunized with 7.5 µg RBD. IgG titers, RBD-specific IgG B cell fractions and NT<sub>50</sub> values were determined from n = 5 biological replicates. One-way ANOVA was performed followed by Dunnett's T3 multiple comparison test at α = 0.05.

249



## 250 References

- 251 1. Singh, A., Eliciting B Cell Immunity against Infectious Diseases Using Nanovaccines. *Nat*  
252 *Nanotechnol* **2021**, *16* (1), 16-24.
- 253 2. Irvine, D. J.; Read, B. J., Shaping Humoral Immunity to Vaccines through Antigen-  
254 Displaying Nanoparticles. *Curr Opin Immunol* **2020**, *65*, 1-6.
- 255 3. Nguyen, B.; Tolia, N. H., Protein-Based Antigen Presentation Platforms for Nanoparticle  
256 Vaccines. *NPJ Vaccines* **2021**, *6* (1), 70.
- 257 4. Zhang, Y. N.; Lazarovits, J.; Poon, W.; Ouyang, B.; Nguyen, L. N. M.; Kingston, B. R.;  
258 Chan, W. C. W., Nanoparticle Size Influences Antigen Retention and Presentation in Lymph Node  
259 Follicles for Humoral Immunity. *Nano Lett* **2019**, *19* (10), 7226-7235.
- 260 5. Batista, F. D.; Iber, D.; Neuberger, M. S., B Cells Acquire Antigen from Target Cells after  
261 Synapse Formation. *Nature* **2001**, *411* (6836), 489-94.
- 262 6. Abbott, R. K.; Lee, J. H.; Menis, S.; Skog, P.; Rossi, M.; Ota, T.; Kulp, D. W.; Bhullar, D.;  
263 Kalyuzhniy, O.; Havenar-Daughton, C.; Schief, W. R.; Nemazee, D.; Crotty, S., Precursor  
264 Frequency and Affinity Determine B Cell Competitive Fitness in Germinal Centers, Tested with  
265 Germline-Targeting Hiv Vaccine Immunogens. *Immunity* **2018**, *48* (1), 133-146 e6.
- 266 7. Marcandalli, J.; Fiala, B.; Ols, S.; Perotti, M.; de van der Schueren, W.; Snijder, J.; Hodge,  
267 E.; Benhaim, M.; Ravichandran, R.; Carter, L.; Sheffler, W.; Brunner, L.; Lawrenz, M.; Dubois, P.;  
268 Lanzavecchia, A.; Sallusto, F.; Lee, K. K.; Velesler, D.; Correnti, C. E.; Stewart, L. J.; Baker, D.;  
269 Lore, K.; Perez, L.; King, N. P., Induction of Potent Neutralizing Antibody Responses by a  
270 Designed Protein Nanoparticle Vaccine for Respiratory Syncytial Virus. *Cell* **2019**, *176* (6), 1420-  
271 1431 e17.
- 272 8. Kato, Y.; Abbott, R. K.; Freeman, B. L.; Haupt, S.; Groschel, B.; Silva, M.; Menis, S.; Irvine,  
273 D. J.; Schief, W. R.; Crotty, S., Multifaceted Effects of Antigen Valency on B Cell Response  
274 Composition and Differentiation in Vivo. *Immunity* **2020**, *53* (3), 548-563 e8.
- 275 9. He, L.; Lin, X.; Wang, Y.; Abraham, C.; Sou, C.; Ngo, T.; Zhang, Y.; Wilson, I. A.; Zhu, J.,  
276 Single-Component, Self-Assembling, Protein Nanoparticles Presenting the Receptor Binding  
277 Domain and Stabilized Spike as Sars-Cov-2 Vaccine Candidates. *Sci Adv* **2021**, *7* (12).
- 278 10. Batista, F. D.; Harwood, N. E., The Who, How and Where of Antigen Presentation to B  
279 Cells. *Nat Rev Immunol* **2009**, *9* (1), 15-27.
- 280 11. Kwak, K.; Akkaya, M.; Pierce, S. K., B Cell Signaling in Context. *Nat Immunol* **2019**, *20*  
281 (8), 963-969.
- 282 12. Gold, M. R.; Reth, M. G., Antigen Receptor Function in the Context of the Nanoscale  
283 Organization of the B Cell Membrane. *Annu Rev Immunol* **2019**, *37*, 97-123.
- 284 13. Dintzis, H. M.; Dintzis, R. Z.; Vogelstein, B., Molecular Determinants of Immunogenicity:  
285 The Immunon Model of Immune Response. *Proc Natl Acad Sci U S A* **1976**, *73* (10), 3671-5.
- 286 14. Tittle, T. V.; Rittenberg, M. B., Igg B Memory Cell Subpopulations: Differences in  
287 Susceptibility to Stimulation by Ti-1 and Ti-2 Antigens. *J Immunol* **1980**, *124* (1), 202-6.
- 288 15. Obukhanych, T. V.; Nussenzweig, M. C., T-Independent Type Ii Immune Responses  
289 Generate Memory B Cells. *J Exp Med* **2006**, *203* (2), 305-10.
- 290 16. Vinuesa, C. G.; Chang, P. P., Innate B Cell Helpers Reveal Novel Types of Antibody  
291 Responses. *Nat Immunol* **2013**, *14* (2), 119-26.
- 292 17. Cerutti, A.; Cols, M.; Puga, I., Marginal Zone B Cells: Virtues of Innate-Like Antibody-  
293 Producing Lymphocytes. *Nat Rev Immunol* **2013**, *13* (2), 118-32.
- 294 18. Crotty, S., T Follicular Helper Cell Biology: A Decade of Discovery and Diseases. *Immunity*  
295 **2019**, *50* (5), 1132-1148.
- 296 19. Victora, G. D.; Nussenzweig, M. C., Germinal Centers. *Annu Rev Immunol* **2022**, *40*, 413-  
297 442.
- 298 20. Cyster, J. G.; Allen, C. D. C., B Cell Responses: Cell Interaction Dynamics and Decisions.  
299 *Cell* **2019**, *177* (3), 524-540.

- 300 21. Boyoglu-Barnum, S.; Ellis, D.; Gillespie, R. A.; Hutchinson, G. B.; Park, Y. J.; Moin, S. M.;  
301 Acton, O. J.; Ravichandran, R.; Murphy, M.; Pettie, D.; Matheson, N.; Carter, L.; Creanga, A.;  
302 Watson, M. J.; Kephart, S.; Ataca, S.; Vaile, J. R.; Ueda, G.; Crank, M. C.; Stewart, L.; Lee, K. K.;  
303 Guttman, M.; Baker, D.; Mascola, J. R.; Veesler, D.; Graham, B. S.; King, N. P.; Kanekiyo, M.,  
304 Quadrivalent Influenza Nanoparticle Vaccines Induce Broad Protection. *Nature* **2021**, *592* (7855),  
305 623-628.
- 306 22. Kanekiyo, M.; Wei, C. J.; Yassine, H. M.; McTamney, P. M.; Boyington, J. C.; Whittle, J.  
307 R.; Rao, S. S.; Kong, W. P.; Wang, L.; Nabel, G. J., Self-Assembling Influenza Nanoparticle  
308 Vaccines Elicit Broadly Neutralizing H1n1 Antibodies. *Nature* **2013**, *499* (7456), 102-6.
- 309 23. Kanekiyo, M.; Bu, W.; Joyce, M. G.; Meng, G.; Whittle, J. R.; Baxa, U.; Yamamoto, T.;  
310 Narpala, S.; Todd, J. P.; Rao, S. S.; McDermott, A. B.; Koup, R. A.; Rossmann, M. G.; Mascola,  
311 J. R.; Graham, B. S.; Cohen, J. I.; Nabel, G. J., Rational Design of an Epstein-Barr Virus Vaccine  
312 Targeting the Receptor-Binding Site. *Cell* **2015**, *162* (5), 1090-100.
- 313 24. Kanekiyo, M.; Joyce, M. G.; Gillespie, R. A.; Gallagher, J. R.; Andrews, S. F.; Yassine, H.  
314 M.; Wheatley, A. K.; Fisher, B. E.; Ambrozak, D. R.; Creanga, A.; Leung, K.; Yang, E. S.; Boyoglu-  
315 Barnum, S.; Georgiev, I. S.; Tsybovsky, Y.; Prabhakaran, M. S.; Andersen, H.; Kong, W. P.; Baxa,  
316 U.; Zephir, K. L.; Ledgerwood, J. E.; Koup, R. A.; Kwong, P. D.; Harris, A. K.; McDermott, A. B.;  
317 Mascola, J. R.; Graham, B. S., Mosaic Nanoparticle Display of Diverse Influenza Virus  
318 Hemagglutinins Elicits Broad B Cell Responses. *Nat Immunol* **2019**, *20* (3), 362-372.
- 319 25. Martinez-Murillo, P.; Tran, K.; Guenaga, J.; Lindgren, G.; Adori, M.; Feng, Y.; Phad, G. E.;  
320 Vazquez Bernat, N.; Bale, S.; Ingale, J.; Dubrovskaya, V.; O'Dell, S.; Pramanik, L.; Spangberg,  
321 M.; Corcoran, M.; Lore, K.; Mascola, J. R.; Wyatt, R. T.; Karlsson Hedestam, G. B., Particulate  
322 Array of Well-Ordered Hiv Clade C Env Trimers Elicits Neutralizing Antibodies That Display a  
323 Unique V2 Cap Approach. *Immunity* **2017**, *46* (5), 804-817 e7.
- 324 26. Akahata, W.; Yang, Z. Y.; Andersen, H.; Sun, S.; Holdaway, H. A.; Kong, W. P.; Lewis, M.  
325 G.; Higgs, S.; Rossmann, M. G.; Rao, S.; Nabel, G. J., A Virus-Like Particle Vaccine for Epidemic  
326 Chikungunya Virus Protects Nonhuman Primates against Infection. *Nat Med* **2010**, *16* (3), 334-8.
- 327 27. Arunachalam, P. S.; Walls, A. C.; Golden, N.; Atyeo, C.; Fischinger, S.; Li, C.; Aye, P.;  
328 Navarro, M. J.; Lai, L.; Edara, V. V.; Roltgen, K.; Rogers, K.; Shirreff, L.; Ferrell, D. E.; Wrenn, S.;  
329 Pettie, D.; Kraft, J. C.; Miranda, M. C.; Kepl, E.; Sydeman, C.; Brunette, N.; Murphy, M.; Fiala, B.;  
330 Carter, L.; White, A. G.; Trisal, M.; Hsieh, C. L.; Russell-Lodrigue, K.; Monjure, C.; Dufour, J.;  
331 Spencer, S.; Doyle-Meyers, L.; Bohm, R. P.; Maness, N. J.; Roy, C.; Plante, J. A.; Plante, K. S.;  
332 Zhu, A.; Gorman, M. J.; Shin, S.; Shen, X.; Fontenot, J.; Gupta, S.; O'Hagan, D. T.; Van Der Most,  
333 R.; Rappuoli, R.; Coffman, R. L.; Novack, D.; McLellan, J. S.; Subramaniam, S.; Montefiori, D.;  
334 Boyd, S. D.; Flynn, J. L.; Alter, G.; Villinger, F.; Kleanthous, H.; Rappaport, J.; Suthar, M. S.; King,  
335 N. P.; Veesler, D.; Pulendran, B., Adjuvanting a Subunit Covid-19 Vaccine to Induce Protective  
336 Immunity. *Nature* **2021**, *594* (7862), 253-258.
- 337 28. Cohen, A. A.; van Doremalen, N.; Greaney, A. J.; Andersen, H.; Sharma, A.; Starr, T. N.;  
338 Keeffe, J. R.; Fan, C.; Schulz, J. E.; Gnanapragasam, P. N. P.; Kakutani, L. M.; West, A. P., Jr.;  
339 Saturday, G.; Lee, Y. E.; Gao, H.; Jette, C. A.; Lewis, M. G.; Tan, T. K.; Townsend, A. R.; Bloom,  
340 J. D.; Munster, V. J.; Bjorkman, P. J., Mosaic Rbd Nanoparticles Protect against Challenge by  
341 Diverse Sarbecoviruses in Animal Models. *Science* **2022**, eabq0839.
- 342 29. Dalvie, N. C.; Rodriguez-Aponte, S. A.; Hartwell, B. L.; Tostanoski, L. H.; Biedermann, A.  
343 M.; Crowell, L. E.; Kaur, K.; Kumru, O. S.; Carter, L.; Yu, J.; Chang, A.; McMahan, K.; Courant,  
344 T.; Lebas, C.; Lemnios, A. A.; Rodrigues, K. A.; Silva, M.; Johnston, R. S.; Naranjo, C. A.; Tracey,  
345 M. K.; Brady, J. R.; Whittaker, C. A.; Yun, D.; Brunette, N.; Wang, J. Y.; Walkey, C.; Fiala, B.; Kar,  
346 S.; Porto, M.; Lok, M.; Andersen, H.; Lewis, M. G.; Love, K. R.; Camp, D. L.; Silverman, J. M.;  
347 Kleanthous, H.; Joshi, S. B.; Volkin, D. B.; Dubois, P. M.; Collin, N.; King, N. P.; Barouch, D. H.;  
348 Irvine, D. J.; Love, J. C., Engineered Sars-Cov-2 Receptor Binding Domain Improves  
349 Manufacturability in Yeast and Immunogenicity in Mice. *Proc Natl Acad Sci U S A* **2021**, *118* (38).

- 350 30. King, H. A. D.; Joyce, M. G.; Lakhali-Naouar, I.; Ahmed, A.; Cincotta, C. M.; Subra, C.;  
351 Peachman, K. K.; Hack, H. R.; Chen, R. E.; Thomas, P. V.; Chen, W. H.; Sankhala, R. S.;  
352 Hajduczki, A.; Martinez, E. J.; Peterson, C. E.; Chang, W. C.; Choe, M.; Smith, C.; Headley, J. A.;  
353 Elyard, H. A.; Cook, A.; Anderson, A.; Wuertz, K. M.; Dong, M.; Swafford, I.; Case, J. B.; Currier,  
354 J. R.; Lal, K. G.; Amare, M. F.; Dussupt, V.; Molnar, S.; Daye, S. P.; Zeng, X.; Barkei, E. K.; Alfson,  
355 K.; Staples, H. M.; Carrion, R.; Krebs, S. J.; Paquin-Proulx, D.; Karasavvas, N.; Polonis, V. R.;  
356 Jagodzinski, L. L.; Vasan, S.; Scott, P. T.; Huang, Y.; Nair, M. S.; Ho, D. D.; de Val, N.; Diamond,  
357 M. S.; Lewis, M. G.; Rao, M.; Matyas, G. R.; Gromowski, G. D.; Peel, S. A.; Michael, N. L.;  
358 Modjarrad, K.; Bolton, D. L., Efficacy and Breadth of Adjuvanted Sars-Cov-2 Receptor-Binding  
359 Domain Nanoparticle Vaccine in Macaques. *Proc Natl Acad Sci U S A* **2021**, *118* (38).
- 360 31. Joyce, M. G.; Chen, W. H.; Sankhala, R. S.; Hajduczki, A.; Thomas, P. V.; Choe, M.;  
361 Martinez, E. J.; Chang, W. C.; Peterson, C. E.; Morrison, E. B.; Smith, C.; Chen, R. E.; Ahmed,  
362 A.; Wiczorek, L.; Anderson, A.; Case, J. B.; Li, Y.; Oertel, T.; Rosado, L.; Ganesh, A.; Whalen,  
363 C.; Carmen, J. M.; Mendez-Rivera, L.; Karch, C. P.; Gohain, N.; Villar, Z.; McCurdy, D.; Beck, Z.;  
364 Kim, J.; Shrivastava, S.; Jobe, O.; Dussupt, V.; Molnar, S.; Tran, U.; Kannadka, C. B.; Soman, S.;  
365 Kuklis, C.; Zemil, M.; Khanh, H.; Wu, W.; Cole, M. A.; Duso, D. K.; Kummer, L. W.; Lang, T. J.;  
366 Muncil, S. E.; Currier, J. R.; Krebs, S. J.; Polonis, V. R.; Rajan, S.; McTamney, P. M.; Esser, M.  
367 T.; Reiley, W. W.; Rolland, M.; de Val, N.; Diamond, M. S.; Gromowski, G. D.; Matyas, G. R.; Rao,  
368 M.; Michael, N. L.; Modjarrad, K., Sars-Cov-2 Ferritin Nanoparticle Vaccines Elicit Broad Sars  
369 Coronavirus Immunogenicity. *Cell Rep* **2021**, *37* (12), 110143.
- 370 32. Yassine, H. M.; Boyington, J. C.; McTamney, P. M.; Wei, C. J.; Kanekiyo, M.; Kong, W.  
371 P.; Gallagher, J. R.; Wang, L.; Zhang, Y.; Joyce, M. G.; Lingwood, D.; Moin, S. M.; Andersen, H.;  
372 Okuno, Y.; Rao, S. S.; Harris, A. K.; Kwong, P. D.; Mascola, J. R.; Nabel, G. J.; Graham, B. S.,  
373 Hemagglutinin-Stem Nanoparticles Generate Heterosubtypic Influenza Protection. *Nat Med* **2015**,  
374 *21* (9), 1065-70.
- 375 33. Jardine, J. G.; Ota, T.; Sok, D.; Pauthner, M.; Kulp, D. W.; Kalyuzhnyi, O.; Skog, P. D.;  
376 Thinnis, T. C.; Bhullar, D.; Briney, B.; Menis, S.; Jones, M.; Kubitz, M.; Spencer, S.; Adachi, Y.;  
377 Burton, D. R.; Schief, W. R.; Nemazee, D., Priming a Broadly Neutralizing Antibody Response to  
378 Hiv-1 Using a Germline-Targeting Immunogen. *Science* **2015**, *349* (6244), 156-61.
- 379 34. Peabody, D. S.; Manifold-Wheeler, B.; Medford, A.; Jordan, S. K.; do Carmo Caldeira, J.;  
380 Chackerian, B., Immunogenic Display of Diverse Peptides on Virus-Like Particles of Rna Phage  
381 Ms2. *J Mol Biol* **2008**, *380* (1), 252-63.
- 382 35. Moon, J. J.; Suh, H.; Li, A. V.; Ockenhouse, C. F.; Yadava, A.; Irvine, D. J., Enhancing  
383 Humoral Responses to a Malaria Antigen with Nanoparticle Vaccines That Expand Tfh Cells and  
384 Promote Germinal Center Induction. *Proc Natl Acad Sci U S A* **2012**, *109* (4), 1080-5.
- 385 36. Walls, A. C.; Fiala, B.; Schafer, A.; Wrenn, S.; Pham, M. N.; Murphy, M.; Tse, L. V.;  
386 Shehata, L.; O'Connor, M. A.; Chen, C.; Navarro, M. J.; Miranda, M. C.; Pettie, D.; Ravichandran,  
387 R.; Kraft, J. C.; Ogohara, C.; Palser, A.; Chalk, S.; Lee, E. C.; Guerriero, K.; Kepl, E.; Chow, C.  
388 M.; Sydeman, C.; Hodge, E. A.; Brown, B.; Fuller, J. T.; Dinnon, K. H., 3rd; Gralinski, L. E.; Leist,  
389 S. R.; Gully, K. L.; Lewis, T. B.; Guttman, M.; Chu, H. Y.; Lee, K. K.; Fuller, D. H.; Baric, R. S.;  
390 Kellam, P.; Carter, L.; Pepper, M.; Sheahan, T. P.; Veessler, D.; King, N. P., Elicitation of Potent  
391 Neutralizing Antibody Responses by Designed Protein Nanoparticle Vaccines for Sars-Cov-2.  
392 *Cell* **2020**, *183* (5), 1367-1382 e17.
- 393 37. Hauser, B. M.; Sangesland, M.; St Denis, K. J.; Lam, E. C.; Case, J. B.; Windsor, I. W.;  
394 Feldman, J.; Caradonna, T. M.; Kannegieter, T.; Diamond, M. S.; Balazs, A. B.; Lingwood, D.;  
395 Schmidt, A. G., Rationally Designed Immunogens Enable Immune Focusing Following Sars-Cov-  
396 2 Spike Imprinting. *Cell Rep* **2022**, *38* (12), 110561.
- 397 38. Herzenberg, L. A.; Tokuhisa, T.; Herzenberg, L. A., Carrier-Priming Leads to Hapten-  
398 Specific Suppression. *Nature* **1980**, *285* (5767), 664-7.

- 399 39. Chackerian, B.; Durfee, M. R.; Schiller, J. T., Virus-Like Display of a Neo-Self Antigen  
400 Reverses B Cell Anergy in a B Cell Receptor Transgenic Mouse Model. *J Immunol* **2008**, *180* (9),  
401 5816-25.
- 402 40. Alonso-Padilla, J.; Papp, T.; Kajan, G. L.; Benko, M.; Havenga, M.; Lemckert, A.; Harrach,  
403 B.; Baker, A. H., Development of Novel Adenoviral Vectors to Overcome Challenges Observed  
404 with Hadv-5-Based Constructs. *Mol Ther* **2016**, *24* (1), 6-16.
- 405 41. Zak, D. E.; Andersen-Nissen, E.; Peterson, E. R.; Sato, A.; Hamilton, M. K.; Borgerding,  
406 J.; Krishnamurty, A. T.; Chang, J. T.; Adams, D. J.; Hensley, T. R.; Salter, A. I.; Morgan, C. A.;  
407 Duerr, A. C.; De Rosa, S. C.; Aderem, A.; McElrath, M. J., Merck Ad5/Hiv Induces Broad Innate  
408 Immune Activation That Predicts Cd8(+) T-Cell Responses but Is Attenuated by Preexisting Ad5  
409 Immunity. *Proc Natl Acad Sci U S A* **2012**, *109* (50), E3503-12.
- 410 42. Rothmund, P. W., Folding DNA to Create Nanoscale Shapes and Patterns. *Nature* **2006**,  
411 *440* (7082), 297-302.
- 412 43. Veneziano, R.; Ratanalert, S.; Zhang, K.; Zhang, F.; Yan, H.; Chiu, W.; Bathe, M.,  
413 Designer Nanoscale DNA Assemblies Programmed from the Top Down. *Science* **2016**, *352*  
414 (6293), 1534.
- 415 44. Knappe, G. A.; Wamhoff, E. C.; Read, B. J.; Irvine, D. J.; Bathe, M., In Situ Covalent  
416 Functionalization of DNA Origami Virus-Like Particles. *ACS Nano* **2021**, *15* (9), 14316-14322.
- 417 45. Jun, H.; Wang, X.; Parsons, M. F.; Bricker, W. P.; John, T.; Li, S.; Jackson, S.; Chiu, W.;  
418 Bathe, M., Rapid Prototyping of Arbitrary 2d and 3d Wireframe DNA Origami. *Nucleic Acids Res*  
419 **2021**, *49* (18), 10265-10274.
- 420 46. Wamhoff, E. C.; Banal, J. L.; Bricker, W. P.; Shepherd, T. R.; Parsons, M. F.; Veneziano,  
421 R.; Stone, M. B.; Jun, H.; Wang, X.; Bathe, M., Programming Structured DNA Assemblies to Probe  
422 Biophysical Processes. *Annu Rev Biophys* **2019**, *48*, 395-419.
- 423 47. Shaw, A.; Hoffecker, I. T.; Smyrlaki, I.; Rosa, J.; Grevys, A.; Bratlie, D.; Sandlie, I.;  
424 Michaelsen, T. E.; Andersen, J. T.; Hogberg, B., Binding to Nanopatterned Antigens Is Dominated  
425 by the Spatial Tolerance of Antibodies. *Nat Nanotechnol* **2019**, *14* (2), 184-190.
- 426 48. Veneziano, R.; Moyer, T. J.; Stone, M. B.; Wamhoff, E. C.; Read, B. J.; Mukherjee, S.;  
427 Shepherd, T. R.; Das, J.; Schief, W. R.; Irvine, D. J.; Bathe, M., Role of Nanoscale Antigen  
428 Organization on B-Cell Activation Probed Using DNA Origami. *Nat Nanotechnol* **2020**, *15* (8),  
429 716-723.
- 430 49. Li, S.; Jiang, Q.; Liu, S.; Zhang, Y.; Tian, Y.; Song, C.; Wang, J.; Zou, Y.; Anderson, G. J.;  
431 Han, J. Y.; Chang, Y.; Liu, Y.; Zhang, C.; Chen, L.; Zhou, G.; Nie, G.; Yan, H.; Ding, B.; Zhao, Y.,  
432 A DNA Nanorobot Functions as a Cancer Therapeutic in Response to a Molecular Trigger in Vivo.  
433 *Nat Biotechnol* **2018**, *36* (3), 258-264.
- 434 50. Wang, Z.; Song, L.; Liu, Q.; Tian, R.; Shang, Y.; Liu, F.; Liu, S.; Zhao, S.; Han, Z.; Sun, J.;  
435 Jiang, Q.; Ding, B., A Tubular DNA Nanodevice as a Sirna/Chemo-Drug Co-Delivery Vehicle for  
436 Combined Cancer Therapy. *Angew Chem Int Ed Engl* **2021**, *60* (5), 2594-2598.
- 437 51. Liu, X.; Xu, Y.; Yu, T.; Clifford, C.; Liu, Y.; Yan, H.; Chang, Y., A DNA Nanostructure  
438 Platform for Directed Assembly of Synthetic Vaccines. *Nano Lett* **2012**, *12* (8), 4254-9.
- 439 52. Lucas, C. R.; Halley, P. D.; Chowdury, A. A.; Harrington, B. K.; Beaver, L.; Lapalombella,  
440 R.; Johnson, A. J.; Hertlein, E. K.; Phelps, M. A.; Byrd, J. C.; Castro, C. E., DNA Origami  
441 Nanostructures Elicit Dose-Dependent Immunogenicity and Are Nontoxic up to High Doses in  
442 Vivo. *Small* **2022**, *18* (26), e2108063.
- 443 53. Dai, L.; Gao, G. F., Viral Targets for Vaccines against Covid-19. *Nat Rev Immunol* **2021**,  
444 *21* (2), 73-82.
- 445 54. Kleanthous, H.; Silverman, J. M.; Makar, K. W.; Yoon, I. K.; Jackson, N.; Vaughn, D. W.,  
446 Scientific Rationale for Developing Potent Rbd-Based Vaccines Targeting Covid-19. *NPJ*  
447 *Vaccines* **2021**, *6* (1), 128.
- 448 55. Walls, A. C.; Park, Y. J.; Tortorici, M. A.; Wall, A.; McGuire, A. T.; Veessler, D., Structure,  
449 Function, and Antigenicity of the Sars-Cov-2 Spike Glycoprotein. *Cell* **2020**.

- 450 56. Yuan, M.; Wu, N. C.; Zhu, X.; Lee, C. D.; So, R. T. Y.; Lv, H.; Mok, C. K. P.; Wilson, I. A.,  
451 A Highly Conserved Cryptic Epitope in the Receptor Binding Domains of Sars-Cov-2 and Sars-  
452 Cov. *Science* **2020**, *368* (6491), 630-633.
- 453 57. Bar-On, Y. M.; Flamholz, A.; Phillips, R.; Milo, R., Sars-Cov-2 (Covid-19) by the Numbers.  
454 *Elife* **2020**, *9*.
- 455 58. Weaver, G. C.; Villar, R. F.; Kanekiyo, M.; Nabel, G. J.; Mascola, J. R.; Lingwood, D., In  
456 Vitro Reconstitution of B Cell Receptor-Antigen Interactions to Evaluate Potential Vaccine  
457 Candidates. *Nat Protoc* **2016**, *11* (2), 193-213.
- 458 59. Wu, Y.; Wang, F.; Shen, C.; Peng, W.; Li, D.; Zhao, C.; Li, Z.; Li, S.; Bi, Y.; Yang, Y.; Gong,  
459 Y.; Xiao, H.; Fan, Z.; Tan, S.; Wu, G.; Tan, W.; Lu, X.; Fan, C.; Wang, Q.; Liu, Y.; Zhang, C.; Qi,  
460 J.; Gao, G. F.; Gao, F.; Liu, L., A Noncompeting Pair of Human Neutralizing Antibodies Block  
461 Covid-19 Virus Binding to Its Receptor Ace2. *Science* **2020**, *368* (6496), 1274-1278.
- 462 60. Hauser, B. M.; Sangesland, M.; Lam, E. C.; Denis, K. J. S.; Feldman, J.; Yousif, A. S.;  
463 Caradonna, T. M.; Kannegieter, T.; Balazs, A. B.; Lingwood, D.; Schmidt, A. G., Engineered  
464 Receptor Binding Domain Immunogens Elicit Pan-Sarbecovirus Neutralizing Antibodies Outside  
465 the Receptor Binding Motif. *bioRxiv* **2021**.
- 466 61. Lingwood, D.; McTamney, P. M.; Yassine, H. M.; Whittle, J. R.; Guo, X.; Boyington, J. C.;  
467 Wei, C. J.; Nabel, G. J., Structural and Genetic Basis for Development of Broadly Neutralizing  
468 Influenza Antibodies. *Nature* **2012**, *489* (7417), 566-70.
- 469 62. Sangesland, M.; Ronsard, L.; Kazer, S. W.; Bals, J.; Boyoglu-Barnum, S.; Yousif, A. S.;  
470 Barnes, R.; Feldman, J.; Quirindongo-Crespo, M.; McTamney, P. M.; Rohrer, D.; Lonberg, N.;  
471 Chackerian, B.; Graham, B. S.; Kanekiyo, M.; Shalek, A. K.; Lingwood, D., Germline-Encoded  
472 Affinity for Cognate Antigen Enables Vaccine Amplification of a Human Broadly Neutralizing  
473 Response against Influenza Virus. *Immunity* **2019**, *51* (4), 735-749 e8.
- 474 63. Saunders, K. O.; Wiehe, K.; Tian, M.; Acharya, P.; Bradley, T.; Alam, S. M.; Go, E. P.;  
475 Scearce, R.; Sutherland, L.; Henderson, R.; Hsu, A. L.; Borgnia, M. J.; Chen, H.; Lu, X.; Wu, N.  
476 R.; Watts, B.; Jiang, C.; Easterhoff, D.; Cheng, H. L.; McGovern, K.; Waddicor, P.; Chapdelaine-  
477 Williams, A.; Eaton, A.; Zhang, J.; Rountree, W.; Verkoczy, L.; Tomai, M.; Lewis, M. G.; Desaire,  
478 H. R.; Edwards, R. J.; Cain, D. W.; Bonsignori, M.; Montefiori, D.; Alt, F. W.; Haynes, B. F.,  
479 Targeted Selection of Hiv-Specific Antibody Mutations by Engineering B Cell Maturation. *Science*  
480 **2019**, *366* (6470).
- 481 64. Jardine, J.; Julien, J. P.; Menis, S.; Ota, T.; Kalyuzhniy, O.; McGuire, A.; Sok, D.; Huang,  
482 P. S.; MacPherson, S.; Jones, M.; Nieusma, T.; Mathison, J.; Baker, D.; Ward, A. B.; Burton, D.  
483 R.; Stamatatos, L.; Nemazee, D.; Wilson, I. A.; Schief, W. R., Rational Hiv Immunogen Design to  
484 Target Specific Germline B Cell Receptors. *Science* **2013**, *340* (6133), 711-6.
- 485 65. McGuire, A. T.; Hoot, S.; Dreyer, A. M.; Lippy, A.; Stuart, A.; Cohen, K. W.; Jardine, J.;  
486 Menis, S.; Scheid, J. F.; West, A. P.; Schief, W. R.; Stamatatos, L., Engineering Hiv Envelope  
487 Protein to Activate Germline B Cell Receptors of Broadly Neutralizing Anti-Cd4 Binding Site  
488 Antibodies. *J Exp Med* **2013**, *210* (4), 655-63.
- 489 66. Corbett, K. S.; Moin, S. M.; Yassine, H. M.; Cagigi, A.; Kanekiyo, M.; Boyoglu-Barnum, S.;  
490 Myers, S. I.; Tsybovsky, Y.; Wheatley, A. K.; Schramm, C. A.; Gillespie, R. A.; Shi, W.; Wang, L.;  
491 Zhang, Y.; Andrews, S. F.; Joyce, M. G.; Crank, M. C.; Douek, D. C.; McDermott, A. B.; Mascola,  
492 J. R.; Graham, B. S.; Boyington, J. C., Design of Nanoparticulate Group 2 Influenza Virus  
493 Hemagglutinin Stem Antigens That Activate Unmutated Ancestor B Cell Receptors of Broadly  
494 Neutralizing Antibody Lineages. *mBio* **2019**, *10* (1).
- 495 67. Ronsard, L.; Yousif, A. S.; Peabody, J.; Okonkwo, V.; Devant, P.; Mogus, A. T.; Barnes,  
496 R. M.; Rohrer, D.; Lonberg, N.; Peabody, D.; Chackerian, B.; Lingwood, D., Engineering an  
497 Antibody V Gene-Selective Vaccine. *Front Immunol* **2021**, *12*, 730471.
- 498 68. Voss, J. E.; Gonzalez-Martin, A.; Andrabi, R.; Fuller, R. P.; Murrell, B.; McCoy, L. E.;  
499 Porter, K.; Huang, D.; Li, W.; Sok, D.; Le, K.; Briney, B.; Chateau, M.; Rogers, G.; Hangartner, L.;

- 500 Feeney, A. J.; Nemazee, D.; Cannon, P.; Burton, D. R., Reprogramming the Antigen Specificity  
501 of B Cells Using Genome-Editing Technologies. *Elife* **2019**, *8*.
- 502 69. Rappuoli, R., Glycoconjugate Vaccines: Principles and Mechanisms. *Sci Transl Med*  
503 **2018**, *10* (456).
- 504 70. Schumann, B.; Hahm, H. S.; Parameswarappa, S. G.; Reppe, K.; Wahlbrink, A.;  
505 Govindan, S.; Kaplonek, P.; Pirofski, L. A.; Witzentrath, M.; Anish, C.; Pereira, C. L.; Seeberger,  
506 P. H., A Semisynthetic Streptococcus Pneumoniae Serotype 8 Glycoconjugate Vaccine. *Sci*  
507 *Transl Med* **2017**, *9* (380).
- 508 71. Tian, J. H.; Patel, N.; Haupt, R.; Zhou, H.; Weston, S.; Hammond, H.; Logue, J.; Portnoff,  
509 A. D.; Norton, J.; Guebre-Xabier, M.; Zhou, B.; Jacobson, K.; Maciejewski, S.; Khatoun, R.;  
510 Wisniewska, M.; Moffitt, W.; Kluepfel-Stahl, S.; Ekechukwu, B.; Papin, J.; Boddapati, S.; Jason  
511 Wong, C.; Piedra, P. A.; Frieman, M. B.; Massare, M. J.; Fries, L.; Bengtsson, K. L.; Stertman, L.;  
512 Ellingsworth, L.; Glenn, G.; Smith, G., Sars-Cov-2 Spike Glycoprotein Vaccine Candidate Nvx-  
513 Cov2373 Immunogenicity in Baboons and Protection in Mice. *Nat Commun* **2021**, *12* (1), 372.
- 514 72. Heath, P. T.; Galiza, E. P.; Baxter, D. N.; Boffito, M.; Browne, D.; Burns, F.; Chadwick, D.  
515 R.; Clark, R.; Cosgrove, C.; Galloway, J.; Goodman, A. L.; Heer, A.; Higham, A.; Iyengar, S.;  
516 Jamal, A.; Jeanes, C.; Kalra, P. A.; Kyriakidou, C.; McAuley, D. F.; Meyrick, A.; Minassian, A. M.;  
517 Minton, J.; Moore, P.; Munsoor, I.; Nicholls, H.; Osanlou, O.; Packham, J.; Pretswell, C. H.; San  
518 Francisco Ramos, A.; Saralaya, D.; Sheridan, R. P.; Smith, R.; Soiza, R. L.; Swift, P. A.; Thomson,  
519 E. C.; Turner, J.; Viljoen, M. E.; Albert, G.; Cho, I.; Dubovsky, F.; Glenn, G.; Rivers, J.; Robertson,  
520 A.; Smith, K.; Toback, S.; nCo, V. S. G., Safety and Efficacy of Nvx-Cov2373 Covid-19 Vaccine.  
521 *N Engl J Med* **2021**, *385* (13), 1172-1183.
- 522 73. Huckriede, A.; Bungener, L.; Daemen, T.; Wilschut, J., Influenza Virosomes in Vaccine  
523 Development. *Methods Enzymol* **2003**, *373*, 74-91.
- 524 74. Morein, B.; Sundquist, B.; Hoglund, S.; Dalsgaard, K.; Osterhaus, A., Iscom, a Novel  
525 Structure for Antigenic Presentation of Membrane Proteins from Enveloped Viruses. *Nature* **1984**,  
526 *308* (5958), 457-60.
- 527 75. Garcia-Beltran, W. F.; Lam, E. C.; Astudillo, M. G.; Yang, D.; Miller, T. E.; Feldman, J.;  
528 Hauser, B. M.; Caradonna, T. M.; Clayton, K. L.; Nitido, A. D.; Murali, M. R.; Alter, G.; Charles, R.  
529 C.; Dighe, A.; Branda, J. A.; Lennerz, J. K.; Lingwood, D.; Schmidt, A. G.; lafrate, A. J.; Balazs,  
530 A. B., Covid-19-Neutralizing Antibodies Predict Disease Severity and Survival. *Cell* **2021**, *184* (2),  
531 476-488 e11.
- 532 76. Garcia-Beltran, W. F.; Lam, E. C.; St Denis, K.; Nitido, A. D.; Garcia, Z. H.; Hauser, B. M.;  
533 Feldman, J.; Pavlovic, M. N.; Gregory, D. J.; Poznansky, M. C.; Sigal, A.; Schmidt, A. G.; lafrate,  
534 A. J.; Naranbhai, V.; Balazs, A. B., Multiple Sars-Cov-2 Variants Escape Neutralization by  
535 Vaccine-Induced Humoral Immunity. *Cell* **2021**, *184* (9), 2523.
- 536 77. Tokatlian, T.; Read, B. J.; Jones, C. A.; Kulp, D. W.; Menis, S.; Chang, J. Y. H.; Steichen,  
537 J. M.; Kumari, S.; Allen, J. D.; Dane, E. L.; Liguori, A.; Sangesland, M.; Lingwood, D.; Crispin, M.;  
538 Schief, W. R.; Irvine, D. J., Innate Immune Recognition of Glycans Targets Hiv Nanoparticle  
539 Immunogens to Germinal Centers. *Science* **2019**, *363* (6427), 649-654.
- 540 78. Tam, H. H.; Melo, M. B.; Kang, M.; Pelet, J. M.; Ruda, V. M.; Foley, M. H.; Hu, J. K.;  
541 Kumari, S.; Crampton, J.; Baldeon, A. D.; Sanders, R. W.; Moore, J. P.; Crotty, S.; Langer, R.;  
542 Anderson, D. G.; Chakraborty, A. K.; Irvine, D. J., Sustained Antigen Availability During Germinal  
543 Center Initiation Enhances Antibody Responses to Vaccination. *Proc Natl Acad Sci U S A* **2016**,  
544 *113* (43), E6639-E6648.
- 545 79. Wamhoff, E. C.; Romanov, A.; Huang, H.; Read, B. J.; Ginsburg, E.; Knappe, G. A.; Kim,  
546 H. M.; Farrell, N. P.; Irvine, D. J.; Bathe, M., Controlling Nuclease Degradation of Wireframe DNA  
547 Origami with Minor Groove Binders. *ACS Nano* **2022**.
- 548 80. Chandrasekaran, A. R., Nuclease Resistance of DNA Nanostructures. *Nat Rev Chem*  
549 **2021**, *5* (4), 225-239.

550 81. Lin-Shiao, E.; Pfeifer, W. G.; Shy, B. R.; Saffari Doost, M.; Chen, E.; Vykunta, V. S.;  
551 Hamilton, J. R.; Stahl, E. C.; Lopez, D. M.; Sandoval Espinoza, C. R.; Deyanov, A. E.; Lew, R. J.;  
552 Poirer, M. G.; Marson, A.; Castro, C. E.; Doudna, J. A., Crispr-Cas9-Mediated Nuclear Transport  
553 and Genomic Integration of Nanostructured Genes in Human Primary Cells. *Nucleic Acids Res*  
554 **2022**, *50* (3), 1256-1268.  
555